Imaging of piezoelectric activity in laser ablated c-axis-oriented LiNbO3/ZnO thin film multilayer on glass using atomic force microscopy

doi: 10.1557/JMR.2003.0284

Imaging of piezoelectric activity in laser-ablated c-axis-oriented $LiNbO_3$/ZnO thin film multilayer on glass using atomic force microscopy

Parmanand Sharma[a] and K. Sreenivas
Department of Physics and Astrophysics, University of Delhi, Delhi 110007, India

L.M. Belova
Department of Materials Science-Tmfy-MSE, Royal Institute of Technology, S-100 44 Stockholm, Sweden, and General Physics Institute, Moscow, 117942, Russia

K.V. Rao
Department of Materials Science-Tmfy-MSE, Royal Institute of Technology, S-100 44 Stockholm, Sweden

(Received 3 March 2003; accepted 1 July 2003)

A $LiNbO_3$/ZnO multilayer with a preferred *c*-axis orientation normal to the plane of the substrate was grown on glass and SiO_2/Si substrates by laser ablation. The piezoelectric activity in as-deposited films was demonstrated using a novel approach to the atomic force microscope. In the presence of an in-plane, low-frequency (0.1–5 Hz) alternating current electric field, we monitored and imaged the induced piezoelectric response normal to the film plane between two electrodes.

Lithium niobate ($LiNbO_3$) is a fascinating material with a valuable combination of piezoelectric and nonlinear optical properties. Many integrated devices can be envisaged if thin films of $LiNbO_3$ can be grown at a lower processing temperature. In-line fiber optic modulators, domain-engineered interfaces for controlled electro-optic deflections,[1] integrated optical waveguide structures,[2] temperature stable surface acoustic wave (SAW)[3] and acousto-optic devices are some of the potential applications.

Epitaxial quality $LiNbO_3$ thin films have been deposited on sapphire and $LiTaO_3$ single-crystal substrates. Optical waveguiding[4] and SAW propagation[5] have been demonstrated. Since $LiNbO_3$ exhibits enhanced properties along specific crystallographic directions, there is a growing interest in finding matched substrate materials, buffer layers, and electrode layers that promote the desired crystallization of $LiNbO_3$. $LiNbO_3$ films with preferred *c*-axis orientation have been reported on silicon (Si) using buffer layers of SiO_2, Si_3N_4, Pt, and/or Al_2O_3 by sputtering,[6–9] while a conducting buffer layer of ZnO on a glass substrates has been used to deposit oriented $LiNbO_3$ films using pulsed-laser ablation.[10] The multilayered structure of $LiNbO_3$/ZnO/SiO_2/Si offers several attractive possibilities because the underlying ZnO buffer layer can be deposited with tailored properties that can provide transparent conducting, insulating, piezoelectric, and electro-optic functions. However, the influence of buffer layer thickness, and actual piezoelectric activity in *c*-axis-oriented $LiNbO_3$ films deposited on Si or glass has not yet been reported.

In recent years, atomic force microscopy (AFM)-based techniques have gained considerable interest in imaging domain structures and in the measurement of small piezoelectric displacements.[11–19] Gruverman *et al.*[12] performed measurements of lead zirconate titanate (PZT) thin films by applying a voltage between a bottom electrode of the sample and a conducting tip of AFM, which acted as a movable electrode. The polarization distribution in PZT thin film was imaged using this configuration. However, the electric field generated by AFM tip was highly inhomogeneous. Alternatively, Christman *et al.*[19] made measurements by applying a voltage between the deposited top and bottom electrode of the sample, and demonstrated a submicrometer variation of piezoelectric properties in PZT capacitors. With this configuration, a homogeneous electric field is generated throughout the piezoelectric layer, and the electrostatic tip–sample interaction was suppressed by the use of a conducting AFM tip. However, in a piezoelectric–metal–piezoelectric structure in thin film form, a dense and a sufficiently thick piezoelectric film becomes necessary to prevent electrical shorting between the top and bottom electrodes.

In this article, we report on the growth of *c* axis-oriented $LiNbO_3$ films using a ZnO buffer layer on glass substrates. The influence of ZnO buffer layers on the crystallization of $LiNbO_3$ is shown to be significant in obtaining an oriented growth of the film. In addition, the

[a]Address all correspondence to this author.
Present address: Institute for Materials Research, Tohoku University, 2-1-1 Katahira, Aoba-Ku, Sendai, 980-8577, Japan.
e-mail: sharmap@imr.tohoku.ac.jp

piezoelectric activity in a *c* axis-oriented $LiNbO_3$/ZnO multilayer has been imaged, in the presence of an applied low-frequency, in-plane potential, by means of the AFM technique.

A $LiNbO_3$/ZnO bilayer was deposited *in situ* on glass (Corning, 7059, Corning, NY) and SiO_2-passivated silicon substrates by a laser-ablation technique. Sintered ceramic targets of [$LiNbO_3$ + 5% excess Li] and ZnO were ablated using a Continuum (model NY81-C) Nd:YAG laser operating in the tripled frequency mode (355 nm) with a pulse-repetition rate of 10 Hz and an energy density of 1.0–1.5 J/cm^2. The substrate temperature (T_s) was varied between 300 °C and 700 °C, while the oxygen pressure during film deposition was maintained at 0.1 mbar. After deposition, the films were slowly cooled in oxygen ambient at the same pressure. The film surface morphology was investigated using a Burleigh AFM. Planar electrodes 2 mm apart were used to study the piezoelectric activity on the surface of the ZnO and $LiNbO_3$ thin films.

Figure 1 shows a typical x-ray diffraction pattern obtained from thin and thick ZnO films deposited at T_s = 450 °C. A peak corresponding to the (002) reflection of ZnO at $2\theta = 34.4°$ confirms the *c*-axis orientation of the film. The inset (a) in Fig. 1 is a plot of the variation in the full width at half maximum (FWHM) of the *(002)* ZnO peak in a 2θ-θ scan for both a thick film (1 μm) and an ultrathin film (~20 nm) as a function of the substrate temperatures during deposition. As seen in Fig. 1 (inset), the FWHM is found to decrease with increasing substrate temperatures, and the figure revealed that the optimum substrate temperature for the growth of *c* axis-oriented ZnO thin films is 400 °C. AFM morphology scans show that the ultrathin ZnO film is continuous with a uniform grain [Fig. 2(a)] and that the grain size is found to increase through the range 1.78–11.34 nm with increasing thickness (20–1000 nm). This increase in the roughness appears to be related to the increase in grain size with film thickness.

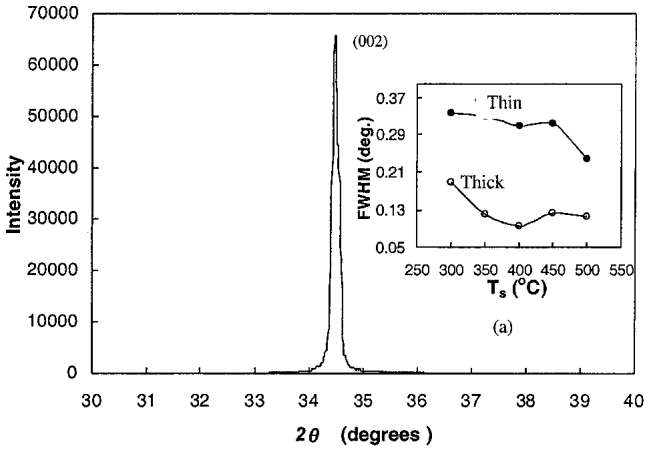

FIG. 1. A typical x-ray diffraction pattern obtained for a ZnO film deposited by laser ablation. (Inset) Variation in FWHM of the (002) peak with T_s for ultrathin and thick ZnO films.

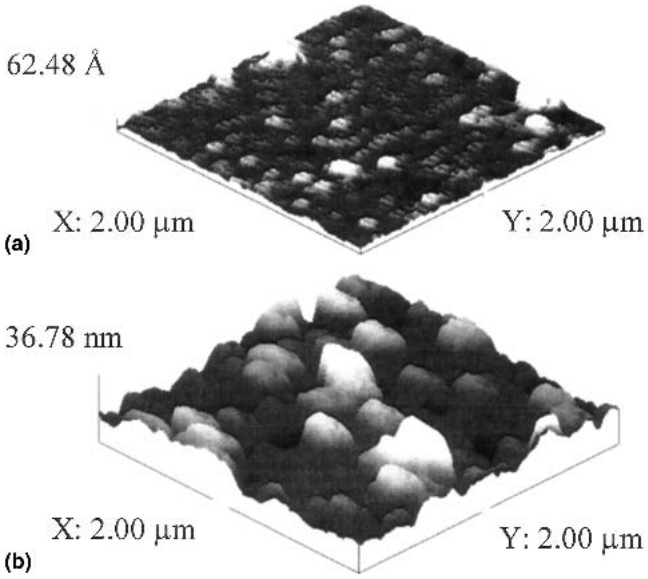

FIG. 2. Surface topography of (a) ultrathin and (b) thick *c* axis-oriented ZnO films.

$LiNbO_3$ films were basically polycrystalline in nature when deposited on a SiO_2/Si substrate at T_s = 500 °C without the ZnO buffer layer [Fig. 3(a)]. However, the overgrowth of $LiNbO_3$ on a *c* axis-oriented ZnO buffer layer (≈20 nm) at T_s = 500 °C clearly exhibited the (006) reflection of $LiNbO_3$ at $2\theta = 39.1°$ [Fig. 3(b)], and could be reproduced on fused quartz and Corning 7059 glass substrates [Fig. 3(c)]. The substrate temperature was critical, and a highly *c* axis-oriented $LiNbO_3$ film on a ZnO buffer layer was obtained for a minimum T_s = 450 °C. The ultrathin ZnO film (20 nm) appears to be adequate to act as a seeding layer for promoting the crystallization of *c*-axis $LiNbO_3$.

The experimental setup for studying the piezoelectric activity in as-grown $LiNbO_3$ and ZnO thin films (thickness 1 μm) is shown in Fig. 4. We have used the AFM to monitor and image the piezoelectric mechanical oscillations normal to the film surface between the points at which an in-plane low frequency electric field is applied. Images were obtained in the contact mode of the AFM using a platinum-coated silicon tip having a cantilever length of 200 μm and a width of 40 μm with a typical force constant of 0.35 N/m. A square or a sine-wave voltage signal of frequency 0.1–5.0 Hz, suitably amplified using a Kepco voltage amplifier (Kepco Inc., NY), was applied between the two planner electrodes (2 mm apart), and scanning was performed between the electrodes. The frequency of the applied signal and the scanning speed of the AFM were selected in such a way as to allow the AFM tip to follow the change in dimensions of

the piezoelectric material with the oscillating electric field. The change in the surface topography (Fig. 5) of the piezoelectric film was found to depend on the frequency and the shape of the applied signal. With an increase in the frequency to 5 Hz, the mechanical vibrations on the film surface were fast and resulted in more periodic oscillations in the scanned image. However, beyond 5 Hz it was difficult to resolve the increasingly large number of mechanical vibrations due to the slow scan speed of the AFM.

In this work, we have shown that it is possible to image the change in dimensions, that is, the change in length perpendicular to the surface, due to the piezoelectric effect when an electric field is applied along the plane of the $LiNbO_3$ or ZnO film. The entire surface between the two electrodes moves up and down, and gives rise to wavelike surface topology in the scanned image. The time taken between the two maxima in the image shown in Fig. 5(a) corresponds well with the time period of the applied voltage signal.

In AFM, the tip of the microscope is known to experience a number of forces. In the present case, in which the response is not observed at the second harmonic, the main forces acting on the tip seem to be due to the applied in-plane electric field and the piezoelectricity

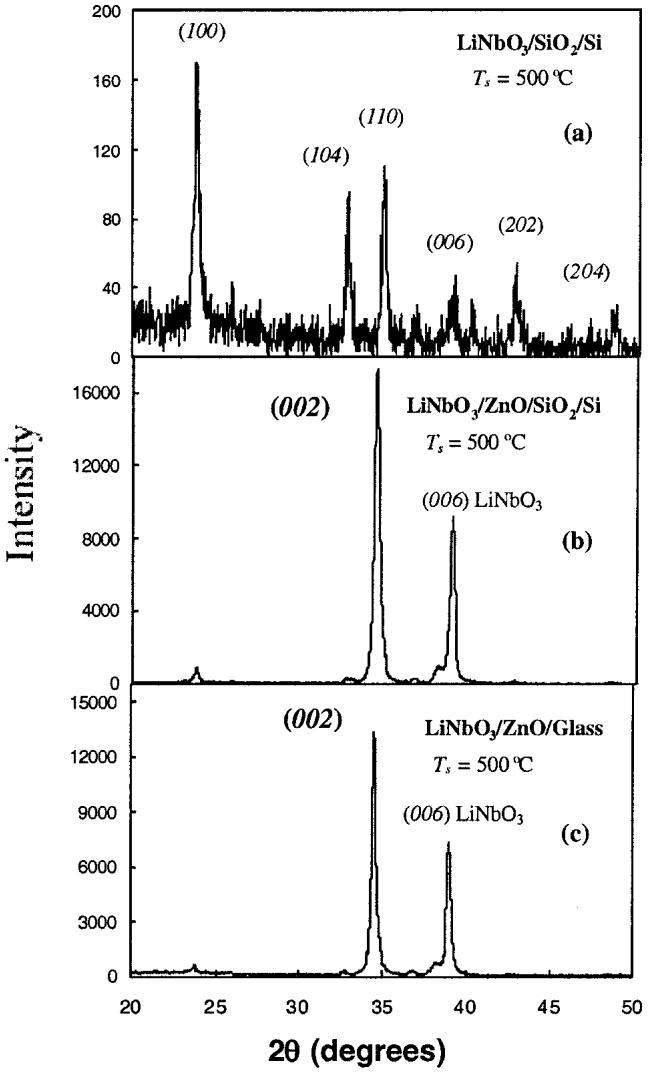

FIG. 3. X-ray diffraction pattern for $LiNbO_3$ thin films (at T_s = 500 °C) (a) $LiNbO_3/SiO_2/Si$ (b) $LiNbO_3/ZnO/SiO_2/Si$, and (c) $LiNbO_3$/ZnO/glass. It shows the effect of the ZnO buffer layer on the crystallization of *c* axis-oriented $LiNbO_3$ thin films grown on different substrates.

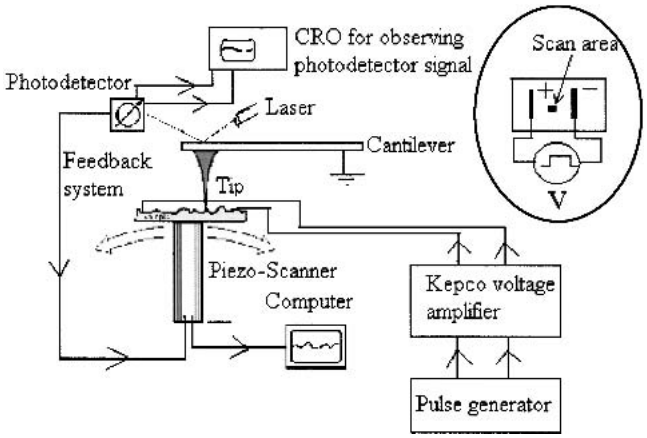

FIG. 4. AFM setup for imaging the piezoelectric response normal to the film surface. (Inset) Sample geometry for generating a piezoelectric response in ZnO and $LiNbO_3$ thin films.

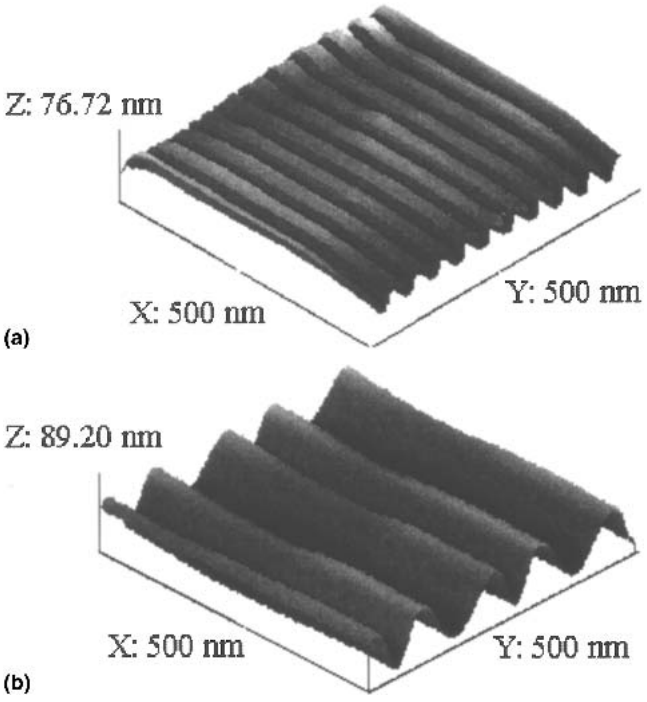

FIG. 5. Surface topography of a $LiNbO_3$/ZnO/glass bilayer in the presence of (a) square-wave and (b) sine-wave electrical signals applied between the planner electrodes (frequency 0.5 Hz). It shows that the surface of a piezoelectric film follows the shape and frequency of the electrical signal.

of the material. The effect of electrostatic interactions between the tip and the film surface was reduced with the use of a conducting tip.[19] A small influence of electrostatic force indeed was observed when the scanning was performed on a bare glass substrate. The inset of Fig. 6 shows the line profile of the AFM image for a glass substrate, and the as-grown *c*-axis-oriented ZnO and/or $LiNbO_3$ thin films in the presence of an in-plane square voltage signal. In the case of a glass substrate [Fig. 6 inset (a)], the displacement of the tip observed due to electrostatic interaction is found to decay even in the presence of an in-plane voltage between the electrodes. In contrast, for a piezoelectric film surface saturation in the tip displacement is observed as long as the exciting in-plane voltage is present [Fig. 6 inset (b)]. The laser-ablated ZnO, $LiNbO_3$, and sputtered ZnO thin films in the present work exhibited similar changes in the topography (Fig. 5), indicating the presence of piezoelectricity. The piezoelectric nature of the sputtered ZnO films was confirmed further by fabricating a SAW delay line.[20] A linear relationship between the tip displacement with the applied voltage for sputtered ZnO, and the as-grown, laser-ablated ZnO and $LiNbO_3$/ZnO is observed (Fig. 6), which is a well-known characteristic of piezoelectric materials. The tip displacement with applied voltage was much larger for the $LiNbO_3$/ZnO structure in comparison to ZnO films and is understood in terms of its relatively large electromechanical coupling coefficient. Beyond 80 V, a significant decrease in tip displacement was observed in the case of laser-ablated ZnO films and might be due to some high-voltage conduction phenomenon. To calculate the piezoelectric constant and to understand the relatively large tip distance with the applied voltage

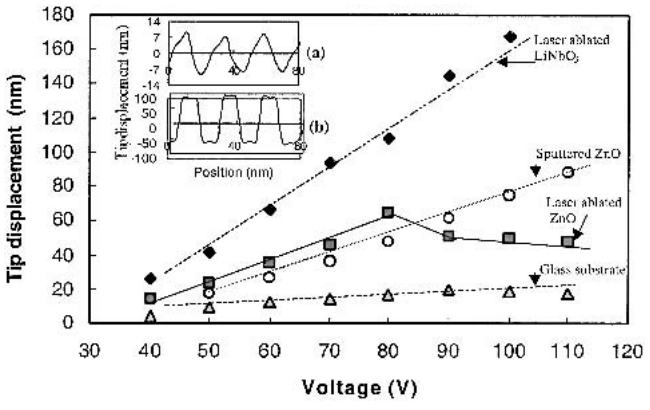

FIG. 6. Variation in tip displacement normal to the film surface in the presence of in-plane applied square voltage signal for (♦) laser-ablated $LiNbO_3$/ZnO/glass, (○) sputtered ZnO/glass, (■) laser-ablated ZnO/glass, and (▲) glass substrate. (Inset) The difference between the responses generated by electrostatic force and that by the piezoelectric force. (a) Line profile of an AFM image showing the decay of tip displacement even in the presence of an in-plane applied voltage between the electrodes on a bare-glass substrate (nonpiezoelectric). (b) Saturation in tip displacement as long as the exciting in-plane voltage is present on the piezoelectric film surface.

observed in the present case requires further investigations, because tip geometry and the type of the feedback system used in the AFM influence the tip displacement.[21,22]

In summary, an optimum thickness of 20 nm of a *c*-axis-oriented ZnO film is found to promote the growth of *c* axis-oriented $LiNbO_3$ films on glass and SiO_2/Si substrates at a minimum substrate temperature of 450 °C. AFM has been used to demonstrate and to image the piezoelectric activity in $LiNbO_3$ and ZnO thin films. A large piezoelectric effect is observed in the laser-ablated $LiNbO_3$/ZnO multilayer in comparison to sputtered and laser-ablated ZnO films.

ACKNOWLEDGMENTS

The authors wish to thank Professor Abhai Mansingh for fruitful discussion, and Ms. Monika Tomar for providing the $LiNbO_3$ target. The authors (P.S. and K.S.) are grateful to the Royal Institute of Technology, Stockholm, Sweden, for the visiting fellowships. (P.S.) wishes to thank Professor Akihisa Inoue for his hospitality and encouragement in this work.

REFERENCES

1. R.W. Eason, A.J. Boyland, S. Mailis, and P.G.R. Smith, Opt. Commun. **197,** 201 (2001).
2. P. Jiang, W. Zhang, and P.J.R. Laybourn, IEEE Proc. **4,** 255 (1990)
3. M. Tomar, V. Gupta, A. Mansingh, and K. Sreenivas, J. Phys. D: Appl. Phys. **34,** 2267 (2001).
4. X. Lansiaux, E. Dogheche, D. Remiens, M. Guilloux-Viry, A. Perrin, and P. Ruterana, J. Appl. Phys. **15,** 5274 (2001).
5. Y. Shibata, K. Kaya, K. Akashi, M. Kanai, T. Kawai, and S. Kawai, Appl. Phys. Lett. **61,** 1000 (1992).
6. S. Tan, T. Gilbert, C-Y. Hung, and T.E. Schlesinger, J. Appl. Phys. **79,** 3548 (1996).
7. S. Tan and T.E. Schlesinger, Appl. Phys. Lett. **68,** 2651 (1996).
8. W.S. Hu, Z.G. Liu, Z.C. Wu, J.M. Liu, X.Y. Chen, and D. Feng, Appl. Surf. Sci. **141,** 197 (1999).
9. M. Shimizu, Y. Furushima, T. Nishida, and T. Shiosaki, Jpn. J. Appl. Phys. **32**(9b), 4111 (1993).
10. J.M. Liu and C.K. Ong, Appl. Phys. A **67,** 493 (1998).
11. K. Franke, J. Besold, W. Haessler, and C. Seegebarth, Surf. Sci. Lett. **302,** L283 (1994).
12. A. Gruverman, O. Auciello, and H. Tokumoto, J. Vac. Sci. Technol., B **14,** 602 (1996).
13. G. Zavala, J.H. Fendler, and S. Trolier-McKinstry, J. Appl. Phys. **81,** 7480 (1997).
14. G.D. Hu, J.B. Xu, and H. Wilson, Appl. Phys. Lett. **75,** 1610 (1999).
15. J. Wittborn, C. Canalias, K.V. Rao, R. Clemens, H. Karlsson, and F. Laurell, Appl. Phys. Lett **80,** 1622 (2002).
16. K. Terabe, S. Takekawa, M. Nakamura, K. Kitamura, S. Higuchi, Y. Gotoh, and A. Gruverman, Appl. Phys. Lett. **81,** 2044 (2002).
17. K. Terabe, M. Nakamura, S. Takekawa, K. Kitamura, S. Higuchi, Y. Gotoh, and Y. Cho, Appl. Phys. Lett. **82,** 433 (2003).
18. B.J. Rodriguez, A. Cruverman, A.I. Kingon, and R.J. Nemanich, Appl. Phys. Lett. **80,** 4166 (2002).
19. J.A. Christman, R.R. Woolcott, A.I. Kingon, and R.J. Nemanich, Appl. Phys. Lett. **73**(26), 3851 (1998).
20. P. Sharma, S. Kumar, and K. Sreenivas, J. Mater. Res. **18,** 545 (2003).
21. V. Kalinin and D.A. Bonnell, Physical Rev. B: Solid State **62,** 10419 (2000).
22. J.W. Yi, W.Y. Shih, and W.H. Shih, J. Appl. Phys. **91,** 1680 (2002).